Signal Processing 167 (2020) 107261

Contents lists available at ScienceDirect

Signal Processing

journal homepage: www.elsevier.com/locate/sigpro

# On the decomposition of multichannel nonstationary multicomponent signals

Ljubiša Stanković[a,*], Miloš Brajović[a], Miloš Daković[a], Danilo Mandic[b]

[a] Faculty of Electrical Engineering, University of Montenegro, Podgorica 81000, Montenegro
[b] Imperial College London, London, United Kingdom

ARTICLE INFO

*Article history:*
Received 20 March 2019
Revised 10 August 2019
Accepted 19 August 2019
Available online 24 August 2019

*Keywords:*
Multivariate and multichannel noisy signals
Time-frequency signal analysis
Robust signal decomposition
Concentration measure

ABSTRACT

With their ability to cater for simultaneously for multifaceted information, multichannel (multivariate) signals have been used to solve problems that are normally not solvable with signals obtained from a single source. One such problem is the decomposition of signals which comprise several components for which the domains of support significantly overlap in both the time, frequency and the joint time-frequency domain. Earlier, we proposed a solution to this problem based on the Wigner distribution of multichannel signals, which requires the attenuation of the cross-terms. In this paper, an advanced solution is proposed, based on eigenvalue analysis of the multichannel signal autocorrelation matrix, followed by the minimization of their time-frequency concentration measure. The analysis offers less restrictive conditions for the signal decomposition, compared to the case of the Wigner distribution. The algorithm for the separation of components is based on concentration measures of the eigenvector time-frequency representation, which represent linear combinations of the overlapping signal components. With an increased number of sensors/channels, the robustness of the decomposition process to additive noise is also demonstrated. The theory is supported by numerical examples, whereby the required channel dissimilarity is also statistically investigated.



## 1. Introduction

It is well established that the use of the conventional Fourier analysis for the characterization and processing of signals with time-varying spectra is quite limited [1–19]. During the last few decades, these constraints have inspired the development of various powerful algorithms and approaches within the time-frequency signal analysis framework [9].

Traditional time-frequency analysis deals with univariate signals, frequently characterized through amplitude and frequency modulated oscillations [9–15,19]. The short-time Fourier transform (STFT) and the Wigner distribution (WD) are commonly used time-frequency representations. In practice, signals are usually multicomponent, meaning that they can be represented as linear combinations of individual signals (components). Owning to its many desirable properties, Wigner distribution has been the basis of many instantaneous frequency (IF) estimators, developed to capture and describe frequency oscillations [9,17,18]. However, undesirable components, known as cross-terms, do appear in the Wigner distribution of multicomponent signals. With the intention to keep desirable properties of the STFT and high concentration of the WD, the S-method is developed as an alternative time-frequency representation, balancing between the previous two [9].

For an independent characterization, each signal (component) in a multicomponent signal should be separated from others and individually analyzed [4–7]. Such decomposition of multicomponent signals on individual components is possible for univariate signals by means of the algorithm originally presented in [4], which is based on the S-method. This type of decomposition is possible under the condition that time-frequency supports of individual components do not overlap. In the univariate case, in general, it is not possible to separate overlapped signal components, except for some very specific and a priori known/assumed signal forms, such as linear frequency modulated signals – using chirplet transform [20] or Radon transform [21], or sinusoidally modulated signals – using inverse Radon transform [22,23].

Recently, new perspectives for the multicomponent signal decomposition have appeared, in light of the multivariate/multichannel signal paradigm [1]. Multivariate (multichannel) data have been largely available lately, as a result of new developments in the sensor technology. With the aim to exploit

* Corresponding author.
*E-mail addresses:* ljubisa@ac.me, l.stankovic@ieee.org (L. Stanković), milosb@ac.me (M. Brajović), milos@ac.me (M. Daković), d.mandic@imperial.ac.uk (D. Mandic).

https://doi.org/10.1016/j.sigpro.2019.107261
0165-1684/

multichannel signal interdependence through a joint time-frequency analysis, concepts of modulated bivariate and trivariate data oscillations appeared first, followed by the generalization of the concept to an arbitrary number of channels [19,24–26]. The joint IF concept has been proposed in [24], as a characterization of multichannel data obtained by capturing combined frequency in all individual channels. The IF of a multichannel signal is defined as a weighted average of the IFs in all individual channels. Following the foundations of these basic time-frequency concepts for the multichannel data, synchrosqueezed transform has been reintroduced within the multivariate/multichannel framework [19]. Furthermore, the wavelet ridge algorithm, as a tool for the extraction of local oscillatory dynamics of multichannel signal, is also defined for multichannel signals [24]. Within the multichannel framework, significant research has also been conducted with the aim to place the empirical mode decomposition within the multichannel/multivariate context [27–31]. Interestingly enough, this type of decomposition is possible only in the case of components which do not overlap in the time-frequency plane, even in the multichannel case.

Multivariate Wigner distribution has been the basis of the recently proposed approach for the decomposition of multichannel multicomponent signals [1]. Exploiting the significant reduction of undesirable cross-terms due to the multichannel signal nature, this method provides the possibility to efficiently extract the components with overlapped supports in the time-frequency domain, something that was not, in general, possible for univariate signals, using any known decomposition procedure. In particular, the autocorrelation matrix of Wigner distribution is decomposed into eigenvectors. Using a steepest descent approach [1], they are linearly combined to form the extracted components. Alongside the possibility to separate overlapped components, it has been even possible to apply the decomposition procedure to extract the IF of real-valued multichannel signals with amplitude variations proportional to phase variations [2]. The influence of channel phase differences (in the bivariate case) is analyzed in [3].

In this paper, the decomposition procedure is performed by starting directly from a realization of signal autocorrelation matrix. This leads to less restrictive signal decomposition conditions, compared to the case of the decomposition based on multichannel Wigner distribution. It is shown that the eigenvectors of the analyzed matrix contains linear combinations of components overlapped in the time-frequency plane. These components are then extracted by minimizing the concentration of the linear combinations of eigenvectors. Numerical results verify the presented theory, with a special emphasis on robustness in noisy conditions and its relation to the number of channels. Overlapped components appear in various signal processing applications, such as in radar signal processing [1], multiple antenna systems [32], some biomedical signals, audio signals [33], to mention but a few. Multivariate time-frequency analysis has been related to the analysis of EEG signals of the newborns [34]. A potentially interesting application of the presented decomposition approach can be also found in multichannel lamb wave analysis [35].

The problem of the multicomponent multichannel signal decomposition can be closely related to the problem of blind source separation [36–38]. Although carrying a similar spirit as the multicomponent signal decomposition considered in this paper, blind source separation based on time-frequency analysis still has some crucial differences. For example, the method for blind source separation proposed in [37] has a different ultimate criterion for the decomposition. Namely, it is based on the difference of time-frequency signatures of the sources, whereas our decomposition approach enforces the separation based on the concentration measure of each individual component. The second difference is the motivation behind the approaches: while the multicomponent multichannel signal decomposition aims at extracting all individual signal components, the blind source separation framework aims to separate signal sources, which could be either monocomponent or multicomponent signals.

The paper organization is as follows. After a short overview of the background theory and basic definitions, Section 2 continues with the detailed analysis of multichannel multicomponent signals. In this section, the attention is devoted to the eigenvectors of signal autocorrelation matrix and their relations with signal components. Section 3 presents the multichannel multicomponent signal decomposition approach, founded on the minimization of the concentration measure. Numerical results are given in Section 4, while the paper ends with concluding remarks.

## 2. Multivariate multicomponent signals

Discrete-time signals of the form

$$\mathbf{x}(n) = \begin{bmatrix} a_1(n)e^{j\phi_1(n)} \\ a_2(n)e^{j\phi_2(n)} \\ \vdots \\ a_C(n)e^{j\phi_C(n)} \end{bmatrix}, \quad n = 1, 2, \ldots, N, \tag{1}$$

obtained by measuring a complex-valued signal $x(n)$ with $C$ sensors, are known as complex multichannel signals. The amplitude and phase of the original signal are modified by each sensor, to give $a_i(n)\exp(j\phi_i(n)) = \alpha_i x(n)\exp(j\varphi_i)$. In the case of real-valued measured signal, its analytic extension

$$x(n) = x_R(n) + j\mathcal{H}\{x_R(n)\}$$

is commonly used, with $x_R(n)$ being the real-valued measured signal and $\mathcal{H}\{x_R(n)\}$ its Hilbert transform. The analytic signal contains only nonnegative frequencies and the real-valued counterpart can be reconstructed. This form of signal is especially important in the instantaneous frequency interpretation within the time-frequency moments framework.

Consider a multichannel signal obtained by sensing a monocomponent signal of the form $x(n) = A(n)\exp(j\psi(n))$. The value of this signal measured at a sensor $i$ can be written as

$$a_i(n)\exp(j\phi_i(n)) = \alpha_i \exp(j\varphi_i)x(n).$$

A real-valued form of this multichannel signal takes the form $a_i(n)\cos(\phi_i(n))$. According to Bedrosian's product theorem [16], the complex analytic signal $a_i(n)\exp(j\phi_i(n)) = a_i(n)\cos(\phi_i(n)) + j\mathcal{H}\{a_i(n)\cos(\phi_i(n))\}$ is a valid representation of the real amplitude-phase signal $a_i(n)\cos(\phi_i(n))$ if the spectrum of $a_i(n)$ is nonzero only within the frequency range $|\omega| < B$ and the spectrum of $\cos(\phi_i(n))$ occupies an nonoverlapping (much) higher frequency range. A signal is monocomponent if $a_i(n)$ is slow-varying as compared to $\phi_i(n)$ variations. The signal model with slow amplitude variations, as compared to the phase variations, has been often considered in literature [39–45].

However, in general, for the case of multicomponent signals, the components are localized along more than one instantaneous frequency.

### 2.1. Multivariate and multicomponent signals

Consider a multicomponent discrete-time signal

$$x(n) = \sum_{p=1}^{P} s_p(n), \tag{2}$$

with $P$ components of the form

$$s_p(n) = A_p(n)e^{j\psi_p(n)}, \tag{3}$$

where the component amplitudes $A_p(n)$ have a slow-varying dynamics as compared to the variations of the phases $\psi_p(n)$. Assume that components are independent signals, i.e., that no component can be written as a linear combination of other components (for all considered time instants $n$). The corresponding multichannel signal is then given by

$$\mathbf{x}(n)=\begin{bmatrix}\sum_{p=1}^{P}\alpha_{1p}s_p(n)e^{j\varphi_{1p}}\\ \sum_{p=1}^{P}\alpha_{2p}s_p(n)e^{j\varphi_{2p}}\\ \vdots\\ \sum_{p=1}^{P}\alpha_{Cp}s_p(n)e^{j\varphi_{Cp}}\end{bmatrix}=\begin{bmatrix}x^{(1)}(n)\\ x^{(2)}(n)\\ \vdots\\ x^{(C)}(n)\end{bmatrix}. \tag{4}$$

Signal in the $m$th channel, denoted by $x^{(m)}(n)$, is obtained as a linear combination of the signal components $s_p(n)$ multiplied with complex constants $a_{mp}=\alpha_{mp}e^{j\varphi_{mp}}$, $m=1,2,\ldots,C$, $p=1,2,\ldots,P$, to give

$$\begin{bmatrix}x^{(1)}(n)\\ x^{(2)}(n)\\ \vdots\\ x^{(C)}(n)\end{bmatrix}=\begin{bmatrix}a_{11}&a_{12}&\ldots&a_{1P}\\ a_{21}&a_{22}&\ldots&a_{2P}\\ \vdots&\vdots&\ddots&\vdots\\ a_{C1}&a_{C2}&\ldots&a_{CP}\end{bmatrix}\begin{bmatrix}s_1(n)\\ s_2(n)\\ \vdots\\ s_P(n)\end{bmatrix}. \tag{5}$$

We will introduce the notation

$$\mathbf{A}=\begin{bmatrix}a_{11}&a_{12}&\ldots&a_{1P}\\ a_{21}&a_{22}&\ldots&a_{2P}\\ \vdots&\vdots&\ddots&\vdots\\ a_{C1}&a_{C2}&\ldots&a_{CP}\end{bmatrix}$$

for the $C\times P$ matrix that transforms the signal components to the measured signal.

*Observation:* The maximum number $M$ of independent channels $x^{(1)}(n)$, $x^{(2)}(n),\ldots,x^{(C)}(n)$ in $\mathbf{x}(n)$ is

$$M=\min\{C,P\}. \tag{6}$$

The proof is evident since the transformation matrix in (4) is an $C\times P$ matrix with $\text{rank}\{\mathbf{A}\}\leq\min\{C,P\}$.

Note that if $C<P$ the maximum number of independent channels $x^{(1)}(n)$, $x^{(2)}(n),\ldots,x^{(C)}(n)$ is equal to the number of sensors $C$, while if $C\geq P$ the maximum number of independent channels is equal to the number of components $P$.

A matrix form of the previous relation between signals measured on $C$ sensors and $P$ signal components is

$$\begin{bmatrix}x^{(1)}(1)&\ldots&x^{(1)}(N)\\ x^{(2)}(1)&\ldots&x^{(2)}(N)\\ \vdots&\ddots&\vdots\\ x^{(C)}(1)&\ldots&x^{(C)}(N)\end{bmatrix}=\mathbf{A}\begin{bmatrix}s_1(1)&\ldots&s_1(N)\\ s_2(1)&\ldots&s_2(N)\\ \vdots&\ddots&\vdots\\ s_P(1)&\ldots&s_P(N)\end{bmatrix}. \tag{7}$$

or

$$\mathbf{X}_{sen}=\mathbf{A}\mathbf{X}_{com}$$

where $\mathbf{X}_{sen}$ is an $C\times N$ matrix of sensed signal values with elements $x^{(s)}(n)$ and $\mathbf{X}_{com}$ is a $P\times N$ matrix of signal component samples with elements $s_p(n)$.

The autocorrelation matrix $\mathbf{R}$ of the sensed signal is defined by

$$\mathbf{R}=\mathbf{X}_{sen}^{H}\mathbf{X}_{sen}, \tag{8}$$

where $(\cdot)^H$ denotes the Hermitian transpose. The elements of this matrix are

$$R(n_1,n_2)=\mathbf{x}^H(n_2)\mathbf{x}(n_1)=\sum_{i=1}^{C}x^{(i)*}(n_2)x^{(i)}(n_1), \tag{9}$$

where $\mathbf{x}(n_1)=[x^{(1)}(n_1)\ x^{(2)}(n_1)\ \ldots\ x^{(C)}(n_1)]^T$ is the column vector of sensed values at a given instant $n_1$.

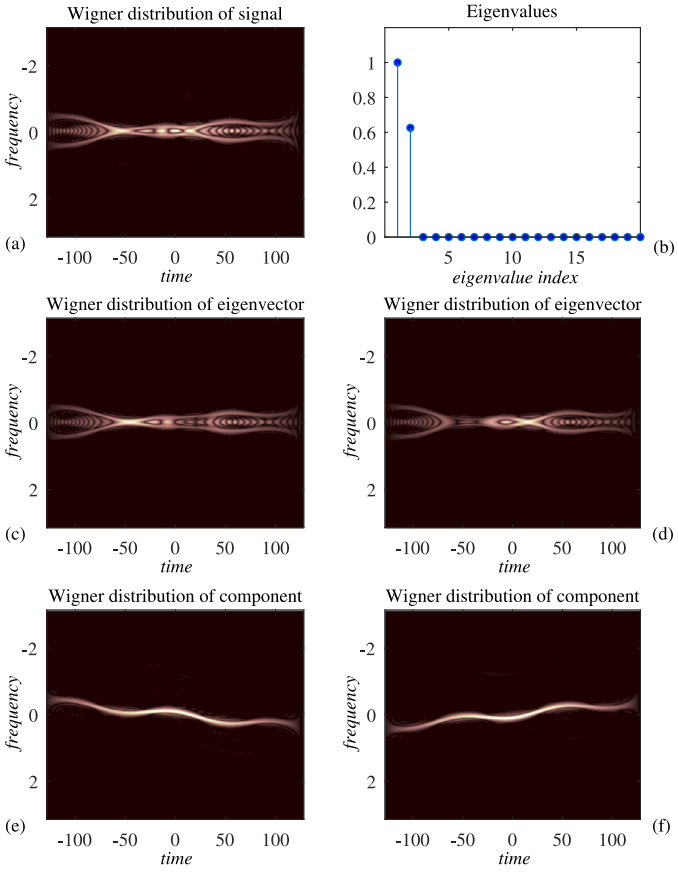


**Fig. 1.** Signal Decomposition with a signal measured by $C=2$ sensors. Additive noise of the standard deviation $\sigma_\epsilon=0.01$ is present in the signal: (a) Time-frequency representation of the input signal. (b) Eigenvalues of the autocorrelation matrix $\mathbf{R}$. (c) Time-frequency representation of the first eigenvector. (d) Time-frequency representation of the second eigenvector. (e) Time-frequency representation of the reconstructed first signal component. (f) Time-frequency representation of the reconstructed second signal component.

The matrix $\mathbf{R}$ can be used for the analysis and characterization of multicomponent multichannel signals. It is also the starting point of the decomposition algorithm for multicomponent signals presented in this paper.

Note that the sensed values $\mathbf{x}(n_1)$ are the linear combinations of the signal components. Although the decomposition could be performed directly, based on the sensed signals, it would not be computationally efficient for $C>P$ that is case common in the analysis. The efficiency is improved using the matrix eigen-decomposition of the autocorrelation matrix $\mathbf{R}$. Some properties of this decomposition, needed for the analysis of multicomponent signals, will be reviewed next.

### 2.2. Eigenvectors and linear combination of vectors

For any square matrix, the eigenvalue decomposition of a $K\times K$ dimensional matrix $\mathbf{R}$ gives

$$\mathbf{R}=\mathbf{Q}\mathbf{\Lambda}\mathbf{Q}^H=\sum_{p=1}^{K}\lambda_p\mathbf{q}_p\mathbf{q}_p^H, \tag{10}$$

where $\lambda_p$ are the eigenvalues and $\mathbf{q}_p$ are the corresponding eigenvectors of $\mathbf{R}$. Matrix $\mathbf{\Lambda}$ is a diagonal matrix with eigenvalues $\lambda_p$, $p=1,\ldots,K$ on the main diagonal whereas the matrix $\mathbf{Q}$ is formed from eigenvectors as $\mathbf{Q}=[\mathbf{q}_1,\ldots,\mathbf{q}_K]$. Note that the eigenvectors $\mathbf{q}_p$ are orthonormal.

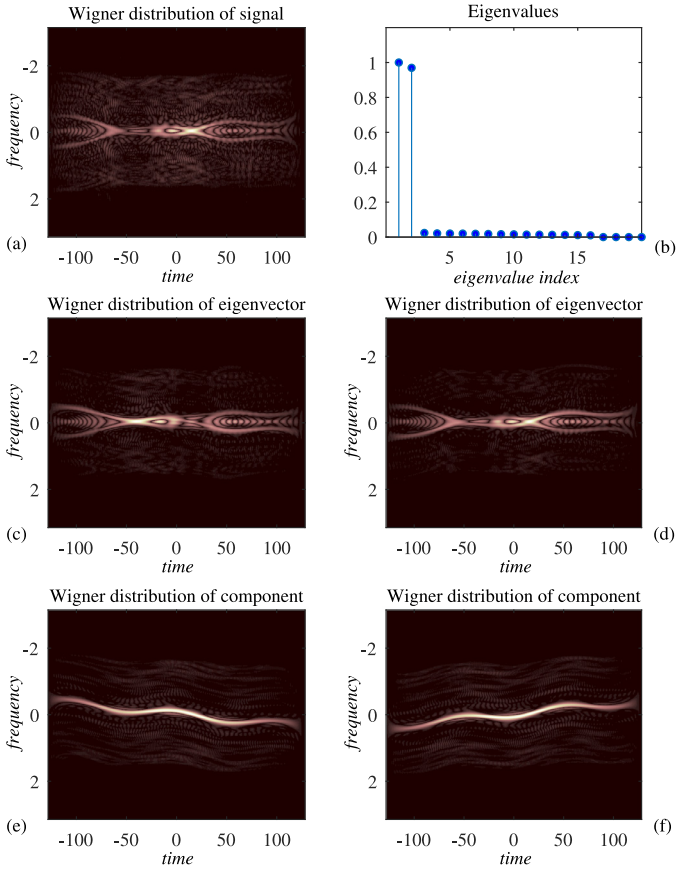


**Fig. 2.** Signal Decomposition with a signal from $C = 16$ sensors. Additive noise of the standard deviation $\sigma_\epsilon = 0.1$ is present in the signal: (a) Time-frequency representation of the input signal. (b) Eigenvalues of the autocorrelation matrix. (c) Time-frequency representation of the first eigenvector. (d) Time-frequency representation of the second eigenvector. (e) Time-frequency representation of the reconstructed first signal component. (f) Time-frequency representation of the reconstructed second signal component.

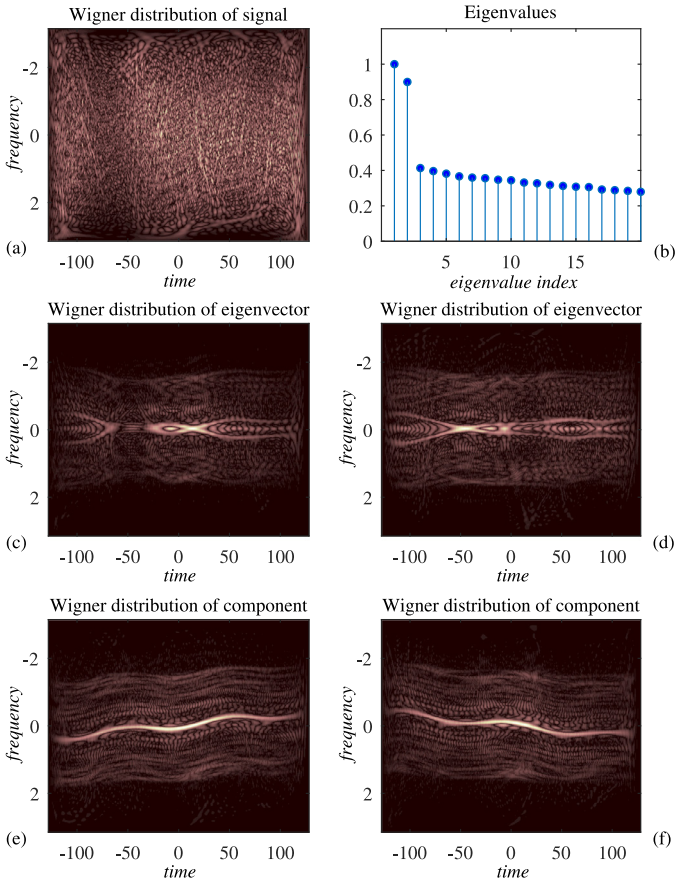


**Fig. 3.** Signal Decomposition with a signal from $C = 128$ sensors. Additive noise of the standard deviation $\sigma_\epsilon = 1$ is present in the signal: (a) Time-frequency representation of the input signal. (b) Eigenvalues of the autocorrelation matrix. (c) Time-frequency representation of the first eigenvector. (d) Time-frequency representation of the second eigenvector. (e) Time-frequency representation of the reconstructed first signal component. (f) Time-frequency representation of the reconstructed second signal component.

**Remark 1.** Consider a set of nonorthogonal vectors $\mathbf{v}_m$, $m = 1, 2, \ldots, M$. If a matrix $\mathbf{R}$ is defined by

$$\mathbf{R} = \sum_{m=1}^{M} \mathbf{v}_m \mathbf{v}_m^H, \tag{11}$$

then finding the eigenvectors of this matrix can be considered as the process of the orthogonalization of the space defined by vectors $\mathbf{v}_m$ whose energies are $\|\mathbf{v}_m\|_2^2 = e_m$.

Note this particular form of matrix is obtained for the multicomponent multichannel overlapping signals, since the elements of matrix $\mathbf{R}$ in (8) are calculated as $R(n_1, n_2) = \mathbf{x}^H(n_2)\mathbf{x}(n_1)$.

The previous remark will be illustrated considering the cases with $M = 1$, $M = 2$, and an arbitrary $M$.

- If $M = 1$ then the orthogonalization over $\mathbf{v}_1$ is not needed. In this case, the eigenvector of matrix $\mathbf{R}$ $\mathbf{q}_1 = \mathbf{v}_1/\sqrt{e_1}$. This case appears exactly if the Wigner distribution is used in univariate signals. This property is used in the synthesis of signals with a given Wigner distribution.
- For $M = 2$, the orthogonalization of the space defined by $\mathbf{v}_1$ and $\mathbf{v}_2$ is performed. In this case, the eigenvectors, $\mathbf{q}_1$, $\mathbf{q}_2$, as the orthogonal vectors over this space, can be written as two linear combinations of $\mathbf{v}_1$ and $\mathbf{v}_2$, that define matrix $\mathbf{R}$ in (11), that is

  $\mathbf{q}_1 = \gamma_{11}\mathbf{v}_1 + \gamma_{21}\mathbf{v}_2$
  $\mathbf{q}_2 = \gamma_{12}\mathbf{v}_1 + \gamma_{22}\mathbf{v}_2$.

  In order to prove this property we will start from definition (11)

  $\mathbf{R} = \mathbf{v}_1\mathbf{v}_1^H + \mathbf{v}_2\mathbf{v}_2^H$.

  We assumed that the eigenvector $\mathbf{q}_1$ is of the form $\mathbf{q}_1 = \gamma_{11}\mathbf{v}_1 + \gamma_{21}\mathbf{v}_2$. The eigenvector of matrix $\mathbf{R}$ satisfies the relation $\mathbf{R}\mathbf{q}_1 = \lambda_1\mathbf{q}_1$. Since

  $$\begin{aligned}\mathbf{R}\mathbf{q}_1 &= (\mathbf{v}_1\mathbf{v}_1^H + \mathbf{v}_2\mathbf{v}_2^H)(\gamma_{11}\mathbf{v}_1 + \gamma_{21}\mathbf{v}_2)\\ &= \mathbf{v}_1\mathbf{v}_1^H(\gamma_{11}\mathbf{v}_1 + \gamma_{21}\mathbf{v}_2) + \mathbf{v}_2\mathbf{v}_2^H(\gamma_{11}\mathbf{v}_1 + \gamma_{21}\mathbf{v}_2)\\ &= \mathbf{v}_1(\gamma_{11}e_1 + \gamma_{21}b_{12}) + \mathbf{v}_2(\gamma_{11}b_{12}^* + \gamma_{21}e_2)\end{aligned}$$

  where $b_{12} = \mathbf{v}_1^H\mathbf{v}_2$, we can obtain a system

  $$\begin{aligned}\lambda_1\mathbf{q}_1 &= \lambda_1(\gamma_{11}\mathbf{v}_1 + \gamma_{21}\mathbf{v}_2)\\ &= \mathbf{v}_1(\gamma_{11}e_1 + \gamma_{21}b_{12}) + \mathbf{v}_2(\gamma_{11}b_{12}^* + \gamma_{21}e_2).\end{aligned}$$

  From this system of equations we can find $\gamma_{11}$, $\gamma_{21}$, and $\lambda_1$, based on $e_1$, $e_2$, and $b_{12}$ with additional condition that $\|\mathbf{q}_1\|_2^2 = 1$. The same holds for $\mathbf{q}_2$.
- This proof can be generalized for any $M$.

  $$\begin{aligned}\mathbf{R}\mathbf{q}_i &= \sum_{m=1}^{M}\mathbf{v}_m\mathbf{v}_m^H\sum_{l=1}^{M}\gamma_{li}\mathbf{v}_l = \sum_{m=1}^{M}\mathbf{v}_m\sum_{l=1}^{M}\gamma_{li}\mathbf{v}_m^H\mathbf{v}_l\\ &= \sum_{m=1}^{M}\mathbf{v}_m\sum_{l=1}^{M}\gamma_{li}b_{ml} = \sum_{m=1}^{M}\mathbf{v}_m B_{mi}\end{aligned}$$

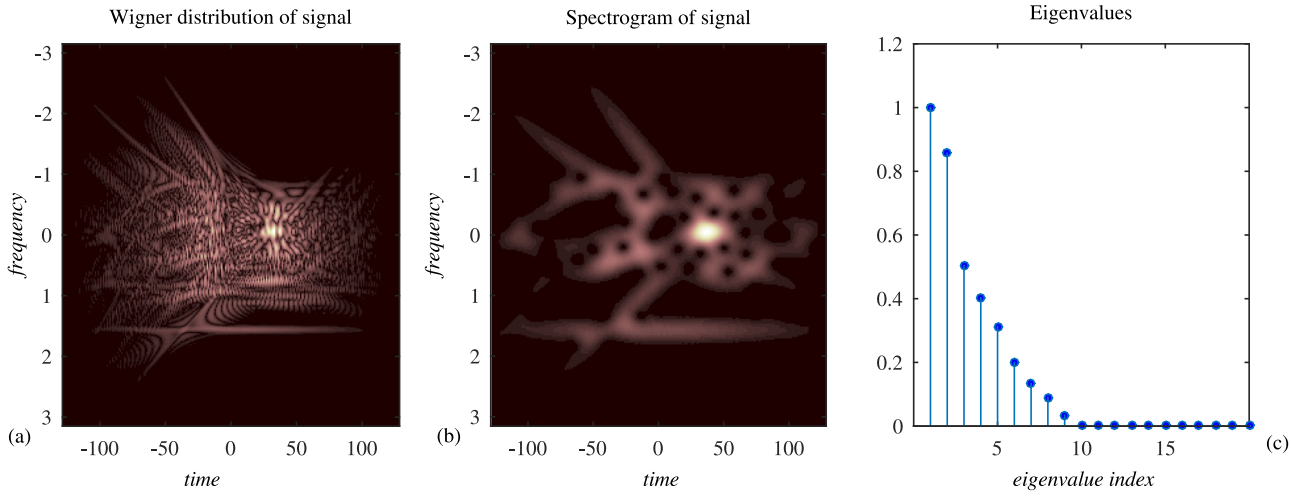


**Fig. 4.** Time-frequency representation of a $P = 9$ component signal using the Wigner distribution (left) and the spectrogram (middle), along with the eigenvectors of the autocorrelation matrix (right) obtained with $C = 12$ sensors. Additive noise of standard deviation $\sigma_\epsilon = 0.01$ is present in the input signal.

From this relation and

$$\lambda_i \mathbf{q}_i = \sum_{m=1}^{M} \mathbf{v}_m \lambda_i \gamma_{mi}$$

with $\mathbf{R}\mathbf{q}_i = \lambda_1 \mathbf{q}_i$ follows the system

$$\sum_{m=1}^{M} \mathbf{v}_m B_{mi} = \sum_{m=1}^{M} \mathbf{v}_m \lambda_i \gamma_{mi}.$$

From this system we may find values of $\gamma_{mi}$ and $\lambda$. Note that $b_{mm} = e_m$ and $b_{ml} = b_{lm}^*$.

**Remark 2.** Assume that

$$\mathbf{R} = \mathbf{v}_1\mathbf{v}_1^H + \mathbf{v}_2\mathbf{v}_2^H + \mathbf{v}_3\mathbf{v}_3^H$$

and that $\mathbf{v}_3$ is not an independent vector, but a linear combination of $\mathbf{v}_1$ and $\mathbf{v}_2$, then

$$\mathbf{q}_1 = \gamma_{11}\mathbf{v}_1 + \gamma_{21}\mathbf{v}_2 + \gamma_{31}\mathbf{v}_3$$
$$\mathbf{q}_2 = \gamma_{12}\mathbf{v}_1 + \gamma_{22}\mathbf{v}_2 + \gamma_{32}\mathbf{v}_3.$$

reduces to

$$\mathbf{q}_1 = \beta_{11}\mathbf{v}_1 + \beta_{21}\mathbf{v}_2$$
$$\mathbf{q}_2 = \beta_{12}\mathbf{v}_1 + \beta_{22}\mathbf{v}_2.$$

It means that a new dependent vector will not increase the dimensionality of the eigenvector space, and it will reduce to a linear combination of the independent vectors, with new coefficients.

**Remark 3.** If the vectors $\mathbf{v}_1$, $\mathbf{v}_2$,...,$\mathbf{v}_M$ are linear combinations of another set of independent vectors $\mathbf{w}_1$, $\mathbf{w}_2$,...,$\mathbf{w}_K$ then the eigenvectors as the linear combinations $\mathbf{v}_1$, $\mathbf{v}_2$,...,$\mathbf{v}_M$ are also the linear combinations of $\mathbf{w}_1$, $\mathbf{w}_2$,...,$\mathbf{w}_K$. For $M = 2$, in the matrix form, for two vectors

$$\begin{bmatrix}\mathbf{q}_1\\ \mathbf{q}_2\end{bmatrix} = \begin{bmatrix}\gamma_{11} & \gamma_{21}\\ \gamma_{12} & \gamma_{22}\end{bmatrix}\begin{bmatrix}\mathbf{v}_1\\ \mathbf{v}_2\end{bmatrix} = \begin{bmatrix}\gamma_{11} & \gamma_{21}\\ \gamma_{12} & \gamma_{22}\end{bmatrix}\begin{bmatrix}\xi_{11} & \xi_{21}\\ \xi_{12} & \xi_{22}\end{bmatrix}\begin{bmatrix}\mathbf{w}_1\\ \mathbf{w}_2\end{bmatrix}$$
$$= \begin{bmatrix}\beta_{11} & \beta_{21}\\ \beta_{12} & \beta_{22}\end{bmatrix}\begin{bmatrix}\mathbf{w}_1\\ \mathbf{w}_2\end{bmatrix}.$$

Therefore, the eigenvectors $\mathbf{q}_m$ are linear combinations of $\mathbf{w}_1$, $\mathbf{w}_2$,...,$\mathbf{w}_K$.

**Remark 4.** If the number of independent vectors $\mathbf{w}_1$, $\mathbf{w}_2$,...,$\mathbf{w}_K$ is $K$ and $\mathbf{v}_1$, $\mathbf{v}_2$,...,$\mathbf{v}_S$, are their linear combinations with $C > K$, then only $K$ vectors $\mathbf{v}_i$ are linearly independent. This means that only $K$ eigenvectors can be formed in this basis.

### 2.3. Eigenvectors as linear combinations of the signal components

The previous remarks represent an analysis platform for our multichannel and multicomponent signal defined by (4). The vectors that form the matrix $\mathbf{R}$ are formed as the following linear combinations of the signal component vectors

$$\mathbf{R} = \mathbf{X}_{sen}^H \mathbf{X}_{sen} = \mathbf{X}_{com}^H \mathbf{A}^H \mathbf{A} \mathbf{X}_{com},$$

with the elements

$$R(n_1, n_2) = \left[s_1^*(n_2),\, s_2^*(n_2),\, \ldots,\, s_P^*(n_2)\right]\mathbf{A}^\mathbf{H}\mathbf{A}\begin{bmatrix}s_1(n_1)\\ s_2(n_1)\\ \vdots\\ s_P(n_1)\end{bmatrix}.$$

The eigenvalue decomposition is then given by

$$\mathbf{R} = \mathbf{Q}\mathbf{\Lambda}\mathbf{Q}^H = \sum_{p=1}^{M} \lambda_p \mathbf{q}_p \mathbf{q}_p^H, \tag{12}$$

where the eigenvectors are linear combinations of $\mathbf{x}^{(i)}$ and these components are linear combinations of the signal components. In other words

$$\mathbf{q}_1 = \alpha_{11}\mathbf{s}_1 + \alpha_{21}\mathbf{s}_2 + \ldots + \alpha_{P1}\mathbf{s}_P$$
$$\mathbf{q}_2 = \alpha_{12}\mathbf{s}_1 + \alpha_{22}\mathbf{s}_2 + \ldots + \alpha_{P2}\mathbf{s}_P$$
$$\vdots$$
$$\mathbf{q}_M = \alpha_{1M}\mathbf{s}_1 + \alpha_{2M}\mathbf{s}_2 + \ldots + \alpha_{PM}\mathbf{s}_P, \tag{13}$$

with $M = \min\{C, P\}$.

Consider the case when the signal components $\mathbf{s}_p(n)$ overlap in the frequency plane. In this case, the decomposition on the individual components is not possible using the state-of-art methods, except in cases of quite specific signal forms (such as linear frequency modulated signals, using chirplet transform, Radon transform or similar techniques [20,21], or for sinusoidally modulated signals using inverse Radon transform, [22,23]). In general, these kinds of signals cannot be separated into individual components in the univariate case. However, the multichannel form of signals offers a possibility to decompose the components which overlap in the time-frequency plane.

## 3. Decomposition principle

We have concluded that the eigenvectors of matrix $\mathbf{R}$ are formed as $M = \min\{C, P\}$ linear combinations of the signal compo-

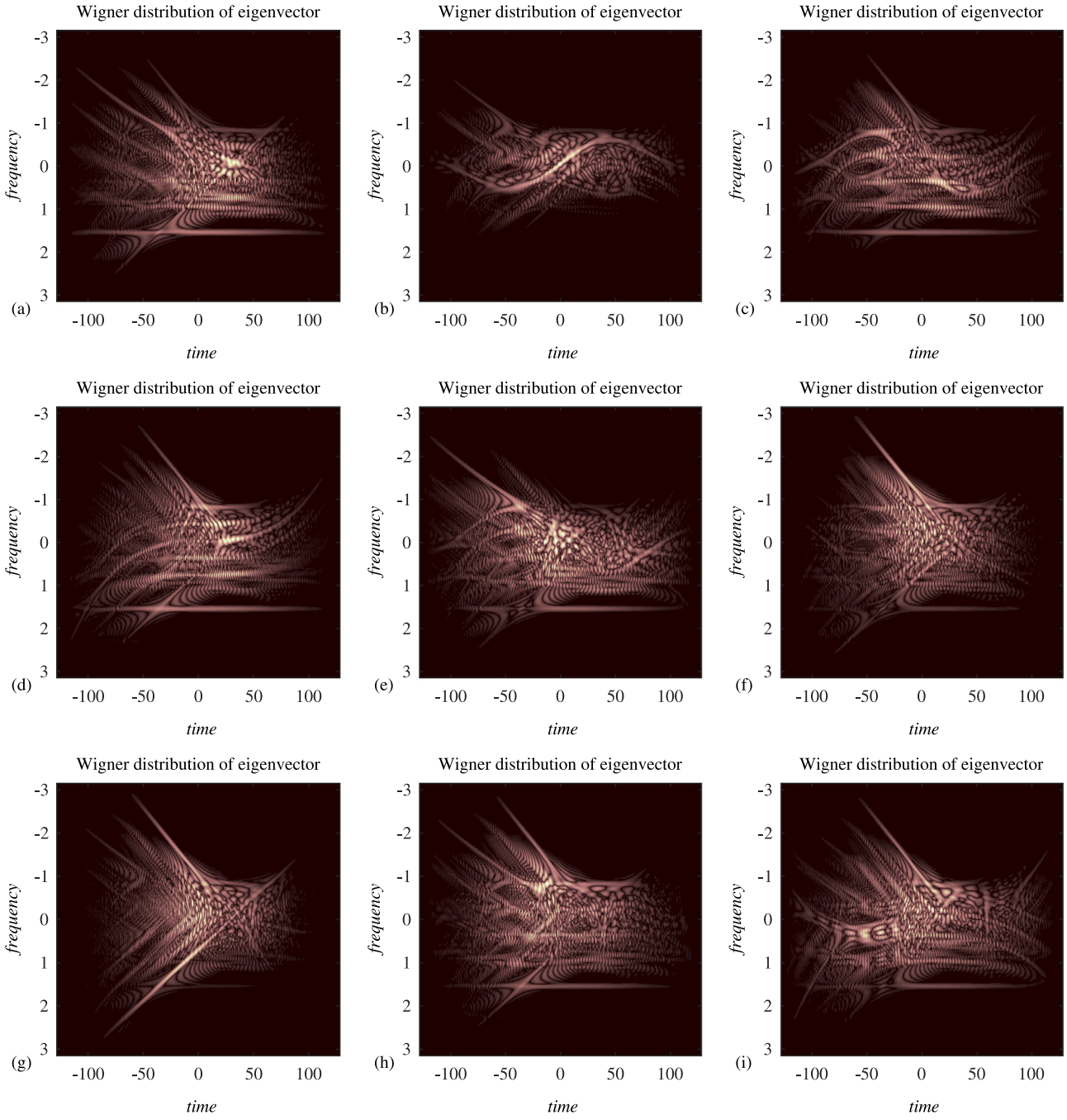


**Fig. 5.** Time-frequency representation of $M = 9$ eigenvectors of the autocorrelation matrix for the signal whose time-frequency representation is shown in Fig. 4.

nents in (13). Assume now that the number of sensors $C$ is such that $C \geq P$. Then there are $M = P$ independent linear relations for $P$ components. We may conclude that, in principle, the signal component $\mathbf{s}_p$ can be also written as linear combination of eigenvectors $\mathbf{q}_p$

$$\mathbf{s}_p = \eta_{1p}\mathbf{q}_1 + \eta_{2p}\mathbf{q}_2 + \ldots + \eta_{Pp}\mathbf{q}_P,$$

with unknown weights $\eta_{ip}$.

We will consider signal with nonstationary components $\mathbf{s}_p$, $p = 1, 2, \ldots, P$. Each component has a support in the time-frequency domain denoted by $\mathbb{D}_p$. For components with partial overlapping, both in time and frequency, the supports also partially overlap. The case with the complete overlapping of two supports is excluded from this analysis. Assume the notation such that $D_1 \leq D_2 \leq \ldots \leq D_P$, where $D_p$ is the area of the support $\mathbb{D}_p$.

The aim of this paper is to decompose the original signal, using the eigenvectors, $\mathbf{q}_p$, $p = 1, 2, \ldots, P$ of autocorrelation matrix $\mathbf{R}$, and to obtain the individual signal components $\mathbf{s}_p$, $p = 1, 2, \ldots, P$, by linearly combining the eigenvectors $\mathbf{q}_p$. To meet this aim, we will use time-frequency representations and corresponding concentration measures. Since the form of time-frequency representation is not crucial here, we will use the short-time Fourier transform (STFT),

$$STFT(n, k) = \sum_{m=0}^{S_w-1} w(m)x(n+m)e^{-j2\pi mk/S_w}, \tag{14}$$

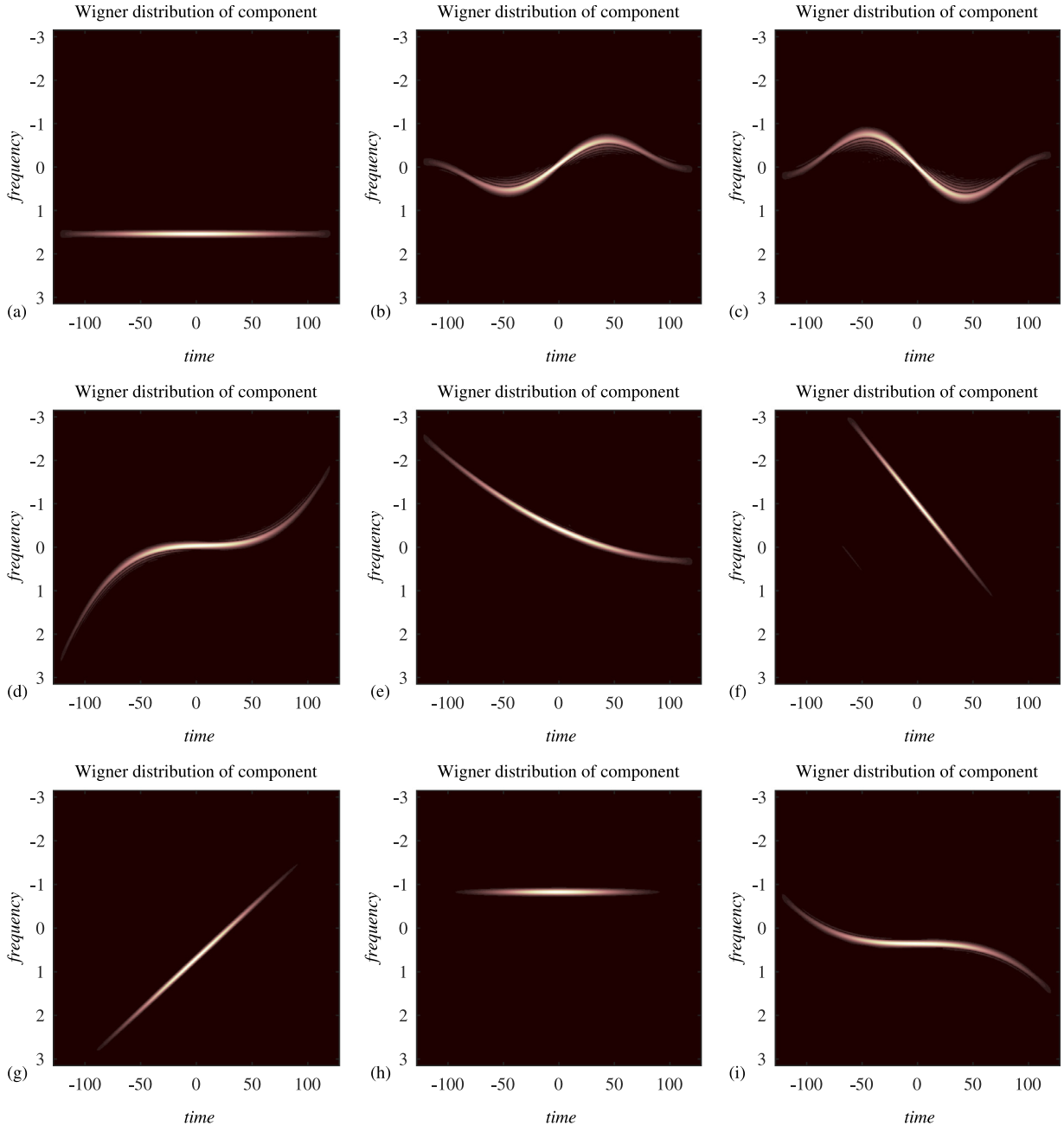


**Fig. 6.** Time-frequency representation of $P = 9$ signal components obtained using the presented algorithm and the eigenvectors from Fig. 5 for the signal whose time-frequency representation is shown in Fig. 4.

to measure the concentration of signals in the time-frequency domain, and the pseudo Wigner distribution

$$WD(n,k) = \sum_{m=0}^{S_w-1} w(m)w(-m)x(n+m)x^*(n-m)e^{-j4\pi\frac{mk}{S_w}}, \qquad (15)$$

to visualize the results, that is, for a high resolution presentation of the initial signal, eigenvectors and the resulting signal components. Note that $w(n)$ denotes a window of length $S_w$ in (14) and (15).

An $L_p$-norm based measure of the time-frequency concentration, with $0 \le p \le 1$, will be used. It is originally introduced in [46] as

$$\mathcal{M}\{STFT(n,k)\} = \|STFT(n,k)\|_p^p \qquad (16)$$

$$= \sum_n \sum_k |STFT(n,k)|^p = \sum_n \sum_k SPEC^{p/2}(n,k), \qquad (17)$$

where $SPEC(n,k) = |STFT(n,k)|^2$ is the spectrogram.

In theory, a direct way to solve the problem of eigenvectors decomposition to the signal components would be to form a linear combination of the eigenvectors

$$\mathbf{y} = \beta_1\mathbf{q}_1 + \beta_2\mathbf{q}_2 + \ldots + \beta_P\mathbf{q}_P, \qquad (18)$$

with varying coefficients $\beta_p$, $p = 1, 2, \ldots, P$, keeping $\|\mathbf{y}\|_2 = const.$, and to use the zero-norm as the concentration measure. This norm would produce the area of the support for the analyzed signal. If all signal components are present in the signal $y(n)$, then its zero-norm would produce the area of $\mathbb{D}_1 \cup \mathbb{D}_2 \cup \ldots \cup \mathbb{D}_P$. By changing the coefficients $\beta_p$, the minimum value of the concentration measure is achieved when the coefficients $\beta_p$ are matched

to the best concentrated signal component coefficients $\eta_{p1}$, $p = 1, 2, \ldots, P$ with the smallest support area $D_1$

$$[\eta_{11}, \eta_{21}, \ldots, \eta_{P1}] = \arg \min_{\beta_1,\ldots,\beta_P} \|SPEC(n,k)\|_0.$$

If any two the smallest areas are equal, we will still find one of them. In practice, the norm-one of the STFT $\|STFT(n,k)\|_1 = \|SPEC(n,k)\|_{1/2}$ could be used to achieve the robustness to noise

$$[\eta_{11}, \eta_{21}, \ldots, \eta_{P1}] = \arg \min_{\beta_1,\ldots,\beta_P} \|STFT(n,k)\|_1. \tag{19}$$

Note that this minimization problem has several local minima as the coefficients $\beta_p$ in $\mathbf{y} = \beta_1\mathbf{q}_1 + \beta_2\mathbf{q}_2 + \ldots + \beta_P\mathbf{q}_P$ which correspond to any signal component $\mathbf{s}_p$ will also produce a local minimum of the concentration measure, equal to the area of corresponding component support. In addition, any linear combination of $K < P$ signal components $\mathbf{s}_p$ will also produce a local minimum equal to the area of the union of the supports of included signal components. Note that if $P$ the lowest local minima correspond to $D_1$, $D_2$,...,$D_P$, then we can detect the coefficients for all signal components.

As several local minima exist, multicomponent decomposition should be performed iteratively. Initially, the matrix $\mathbf{R}$ with elements (9) is calculated as in (8). Its eigen-decomposition produces eigenvectors $\mathbf{q}_p$, $p = 1, 2, \ldots, P$, and based on them, signal

$$\mathbf{y} = \beta_1\mathbf{q}_1 + \beta_2\mathbf{q}_2 + \ldots + \beta_P\mathbf{q}_P$$

is formed, with weighting coefficients $\beta_p$, $p = 1, 2, \ldots, P$, which are varied to solve the minimization problem (19). The STFT in (19) is calculated for the normalized signal $\mathbf{y}/\|\mathbf{y}\|_2 = \mathbf{y}/\|\sum_{p=1}^{P}\beta_p\mathbf{q}_p\|_2$. Here, we can assume that the minimization (19) is performed by the direct search over the parameter space.

The direct search procedure is simple, but it is not computationally efficient. It assumes that real and imaginary parts of each parameter $\beta_1, \beta_2, \ldots, \beta_P$, originally initialized by zero values, are varied over the intervals $[-1, 1]$ with a step $\mu$, aiming to find the combination of parameter values that produces the minimum of the concentration measure. The search space is limited to these intervals because the concentration measure is calculated for the normalized signal $\mathbf{y}/\|\mathbf{y}\|_2$ with unit energy, and eigenvectors are orthonormal (of unit energy) by definition. The choice of the step $\mu$ is a matter of compromise between the execution time and precision. Note that in one iteration of the decomposition algorithm (for the $i$th eigenvector), the search space dimension is $2P - 2$, as $\beta_i = 1$ holds.

The search in the space of parameters $\beta_1, \beta_2, \ldots, \beta_P$, in order to minimize the measure $\mathcal{M}\{STFT(n,k)\} = \|STFT_y(n,k)\|_1$ can be also performed by using more sophisticated methods, such as the iterative gradient minimization procedure presented in [1]. Other global optimization methods, including heuristic algorithms - ant colony optimization [47], genetic algorithm, hill climbing [48], simulated annealing [49], and also, using some deterministic [50] or stochastic procedures [51,52], can be also used for the concentration measure minimization.

Upon finding the concentration measure minimum, the eigenvector $\mathbf{q}_1$ is replaced with the signal $\mathbf{s}_1 = \eta_{11}\mathbf{q}_1 + \eta_{21}\mathbf{q}_2 + \ldots + \eta_{P1}\mathbf{q}_P$, formed using the weighting coefficients corresponding to the minimum of concentration measure (19). Then, this signal is removed from the remaining eigenvectors, by removing its projection to these eigenvectors. In other words, the eigenvectors $\mathbf{q}_p$, $p = 2, 3, \ldots, P$, are modified as follows:

$$\mathbf{q}_p = \frac{\mathbf{q}_p - \mathbf{q}_1^H\mathbf{q}_p\mathbf{q}_1}{\sqrt{1 - |\mathbf{q}_1^H\mathbf{q}_p|^2}}, \tag{20}$$

in order to ensure that $\mathbf{s}_1$ it is not detected again.

This procedure is iterated $P$ times. This means that in the $i$th iteration, based on eigenvectors $\mathbf{q}_p$ modified in the previous iteration, new signal

$$\mathbf{y} = \sum_{p=1}^{P}\beta_p\mathbf{q}_p, \tag{21}$$

is formed. The weighting coefficients $\beta_p$, $p = 1, 2, \ldots, P$ are varied, to find the new set $\eta_{1i}, \eta_{2i}, \ldots, \eta_{Pi}$ which minimizes the concentration measure

$$[\eta_{1i}, \eta_{2i}, \ldots, \eta_{Pi}] = \arg \min_{\beta_1,\ldots,\beta_P} \|STFT_y(n,k)\|_1,$$

of the spectrogram calculated for normalized current signal $\mathbf{y}/\|\mathbf{y}\|_2$. Here, $STFT_y(n, k)$ stands for the short-time Fourier transform of signal $\mathbf{y}/\|\mathbf{y}\|_2$ calculated according to (14). The $i$-th eigenvector is replaced by $\mathbf{s}_i = \eta_{1i}\mathbf{q}_1 + \eta_{2i}\mathbf{q}_2 + \ldots + \eta_{Pi}\mathbf{q}_P$, while the signal deflation [53] is performed by subtracting the projection of the detected component from remaining eigenvectors $\mathbf{q}_p$, $p = i+1, i+2, \ldots, P$:

$$\mathbf{q}_p = \frac{\mathbf{q}_p - \mathbf{q}_i^H\mathbf{q}_p\mathbf{q}_i}{\sqrt{1 - |\mathbf{q}_i^H\mathbf{q}_p|^2}}. \tag{22}$$

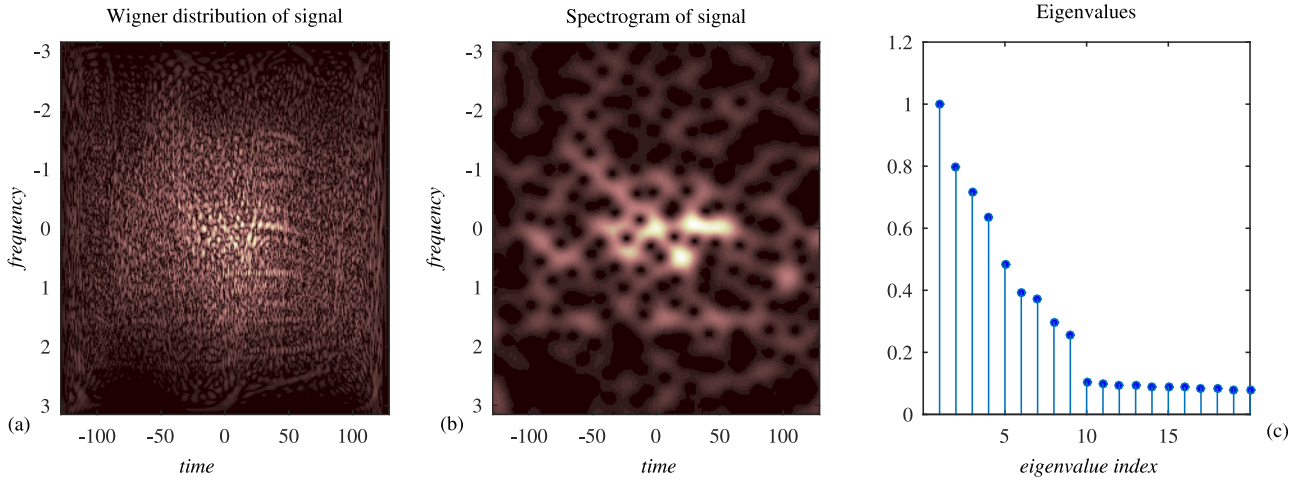


**Fig. 7.** Time-frequency representation of a $P = 9$ component signal using the Wigner distribution (left) and the spectrogram (middle), along with the eigenvectors of the autocorrelation matrix (right) obtained with $C = 128$ sensors. Additive noise of standard deviation $\sigma_\epsilon = 1$ is present in the input signal.

The described procedure is repeated until there is no more updates of vectors $\mathbf{q}_p$. Vectors $\mathbf{q}_p$ are sorted according to their concentration measure, after each iteration. The iterative procedure is stopped when there is no updates of vectors $\mathbf{q}_p$. Although repeating the procedure as long as eigenvector updates exist is numerically less efficient, it prevents the effect of error propagation and at the same time it also prevents the possibility that a linear combination of eigenvectors, producing a local minimum, is detected as a component.

In the noisy signal cases, the number of components can be determined based on two approaches: (a) The number of components is assumed. As long as it is larger than or equal to the true number of components $P$, the algorithm works properly, producing noise only as the extra components; (b) A threshold is set to separate eigenvalues corresponding to signal components from those corresponding to the noise. This threshold determines the number of components in the decomposition.

### 3.1. Specific cases

When the components do not overlap in the time-frequency plane, they are orthogonal. If the number of sensors is greater or equal to the number of components, $C \geq P$, then the components are equal to the eigenvectors (up to their amplitudes) and the decomposition directly follows. In sense of the previous equations it means that we can use $b_{mn} = 0$ for $m \neq n$.

This problem can be solved even if single signal channel is available, $C = 1$, by using time-frequency representation of the

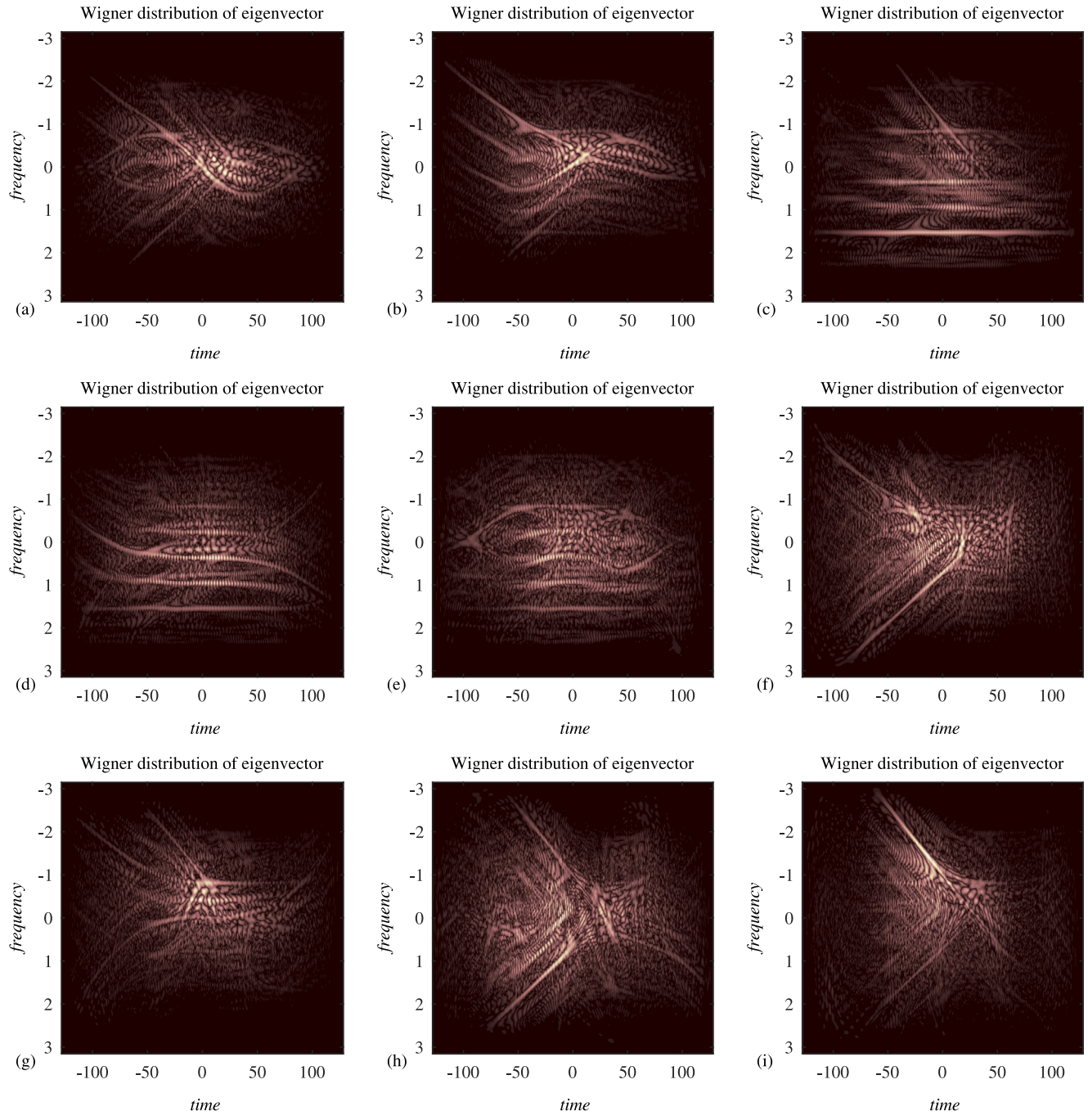


**Fig. 8.** Time-frequency representation of $M = 9$ eigenvectors of the autocorrelation matrix for the noisy signal whose time-frequency representation is shown in Fig. 7.

signal which produces the cross-terms free Wigner distribution – the S-method, [4].

The case of combined $P_o$ overlapping and $P_n$ nonoverlapping components, $P = P_o + P_n$ can be solved with at least $C = P_o$ sensors, as shown in [1].

## 4. Numerical examples

This section supports the theory by on numerical examples. In Examples 1–3, a real-valued discrete-time bivariate signal with overlapping components is considered with various noise amounts (variances). This set of examples confirms the fact that in order to perform an efficient decomposition in noisy cases – the number of channels should be increased, compared with the noiseless scenario. In Examples 4–5, a very complex signal of nine overlapping components is considered, corrupted with noise with two different levels. The analysis is concluded with a statistical test which will illustrate how the ability to separate the components depends on the noise variance and the number of channels.

**Example 1.** Consider a discrete-time bivariate signal of the form $\mathbf{x}(n) = [s_1(n),\ s_2(n)]^T$. The minimum required number of sensors for this signal, $C = 2$, is used. Signal from the channel $i$ is of the form

$$x^{(i)}(n) = e^{-(n/128)^2} \cos\left(2\sin\left(5\pi\frac{n}{N}\right) - 2\pi\frac{n^2}{16N} + \varphi_i\right) \tag{23}$$

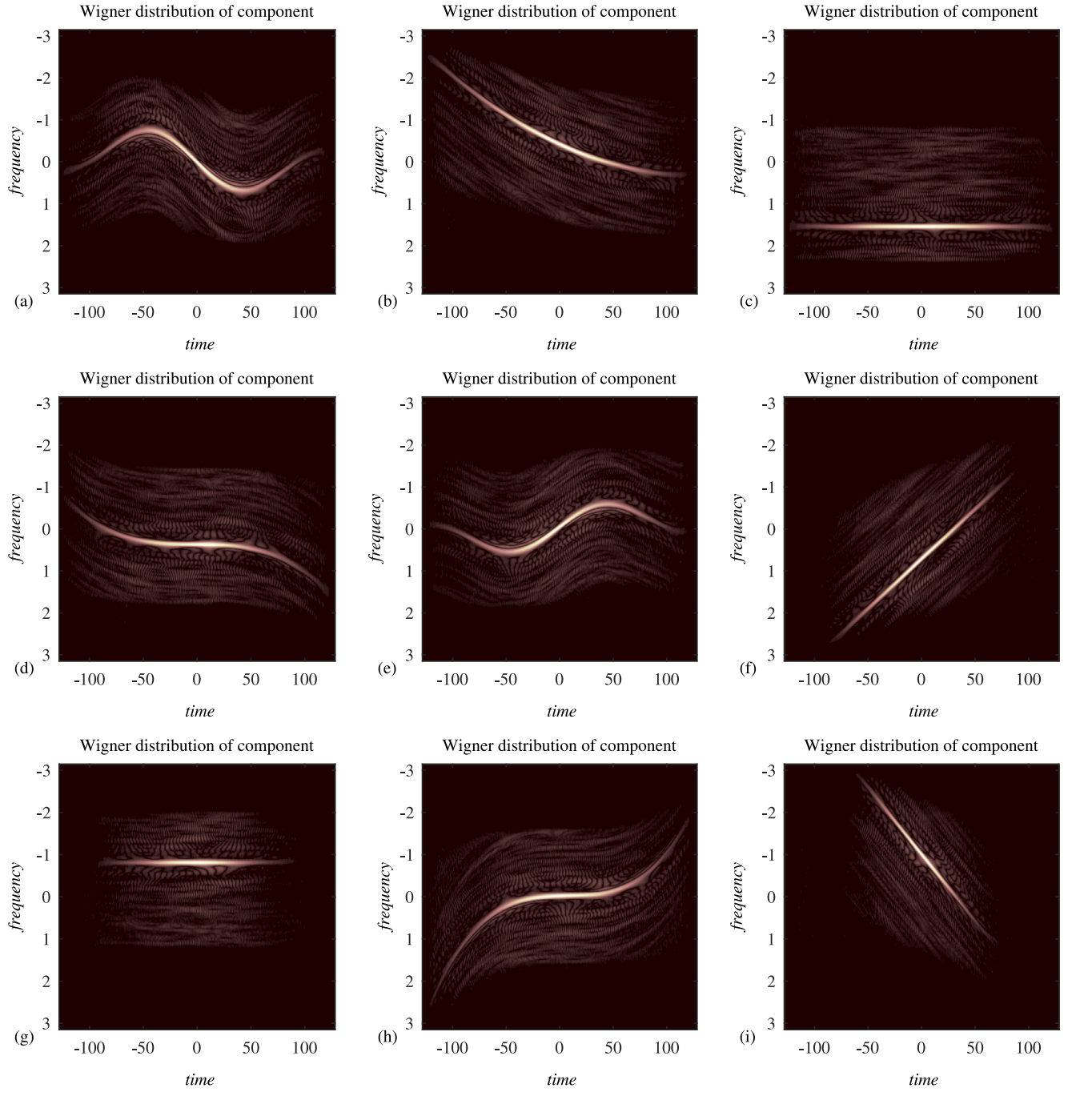


**Fig. 9.** Time-frequency representation of $P = 9$ signal components obtained using the presented algorithm and the eigenvectors from Fig. 8 for the noisy signal whose time-frequency representation is shown in Fig. 7.

for $-128 \leq n \leq 128$ and $N = 257$, as shown in Fig. 1. The components of this signal are

$$s_{1,2}^{(i)}(n) = e^{-(n/128)^2} e^{\pm j2\sin(5\pi\frac{n}{N}) - j2k\pi\frac{n^2}{16N} + j\varphi_i}. \quad (24)$$

Time-frequency representation of this signal with two very close components is shown in Fig. 1(a). The eigenvectors of the autocorrelation matrix indicate that there are two signal components, as shown in Fig. 1(b). The two eigenvectors corresponding to the largest eigenvalues are presented in Fig. 1(c)–(d). These two eigenvectors are decomposed into two signal components with minimum concentration measures, as described in the previous section. The decomposition results are shown in Fig. 1(e)–(f), and they fully correspond to the time-frequency representation of the individual signal components in (24).

**Example 2.** The signal from Example 1 is corrupted by a moderate level of additive noise, to give $x^{(i)}(n) + \varepsilon^{(i)}(n)$. The standard deviation of noise is $\sigma_\varepsilon = 0.1$. Here, we were not able to reconstruct the signal with the minimum number of sensors. To achieve a stable reconstruction, the number of sensors is increased to $C = 16$. The time-frequency representation of the original noisy signal, eigenvalues, time-frequency representation of the eigenvectors, and the time-frequency representation of the obtained signal components are shown in Fig. 2.

**Example 3.** In this case the noise intensity is increased to the signal level using $\sigma_\varepsilon = 1$. To achieve robustness of the results, the number of sensors had to be increased. Noisy signal time-frequency representation, along with eigenvalues, time-frequency representation of the eigenvectors, and the time-frequency representation of the signal components are presented in Fig. 3.

**Example 4.** In this example, a signal with a large number of $P = 9$ overlapped components is considered. The minimum number of sensors, required for the successful decomposition is $C = P = 9$ in this case. Since a small noise is added, with $\sigma_\varepsilon = 0.01$, and the measured signal phases are random, the signal is reconstructed with a small margin in the number of sensors $C = 12$. From the time-frequency representation of components, presented in Fig. 4(a)–(b), we can see that the components overlapping is significant. Components cannot be recognized neither from the Wigner distribution nor from the spectrogram with an adjusted window. Their eigenvalues of the autocorrelation matrix are shown in Fig. 4(c). The time-frequency representation of the strongest 9 eigenvectors are presented in Fig. 5. Using these eigenvectors the signal is decomposed into components, as shown in Fig. 6.

**Example 5.** A noisy signal, as in Example 4, with $P = 9$ components is analyzed here. In addition to the random different phases in each sensor, a random amplitude change is assumed as well. The coefficients in (4) defined by $a_{mp} = \alpha_{mp} e^{j\varphi_{mp}}$, are here used in the form $a_{mp} = (1 + \nu_{mn})\alpha_{mp} e^{j\varphi_{mp}}$, where the random variable $\nu_{mn}$ assume the values within $-0.25 \leq \nu_{mn} \leq 0.25$ and the variable $\varphi_{mp}$ is uniformly distributed over the interval from 0 to $2\pi$. The decomposition results are presented in the same way as in the previous figures. Time-frequency representations obtained using the Wigner distribution and the spectrogram are given in Fig. 7, along with the eigenvalues of the autocorrelation matrix. The time-frequency representations of the 9 strongest eigenvectors are shown in Fig. 8. The linear combinations of the eigenvectors are done according to the presented algorithm and the final results for the signal components can be seen in Fig. 9.

Finally, a statistical test is run for the noisy $P = 9$ component signal from the last example. The eigenvalues are calculated in 1000 random realizations and presented in Fig. 10 for two values of the additive noise variance $\sigma_\varepsilon^2 = 1$ and $\sigma_\varepsilon^2 = 1/2$. Ability to clearly separate the strongest $P = 9$ eigenvectors, corresponding to the linear combinations of the signal components, from the background noise is a good indicator when the presented algorithm can successfully be applied. For the value of variance $\sigma_\varepsilon^2 = 1/2$ we can conclude that the number of sensors $C > 50$ would be sufficient, while the same separation gap is obtained for $C > 100$ with $\sigma_\varepsilon^2 = 1$. This indicator is verified against the reconstruction check for these scenarios.

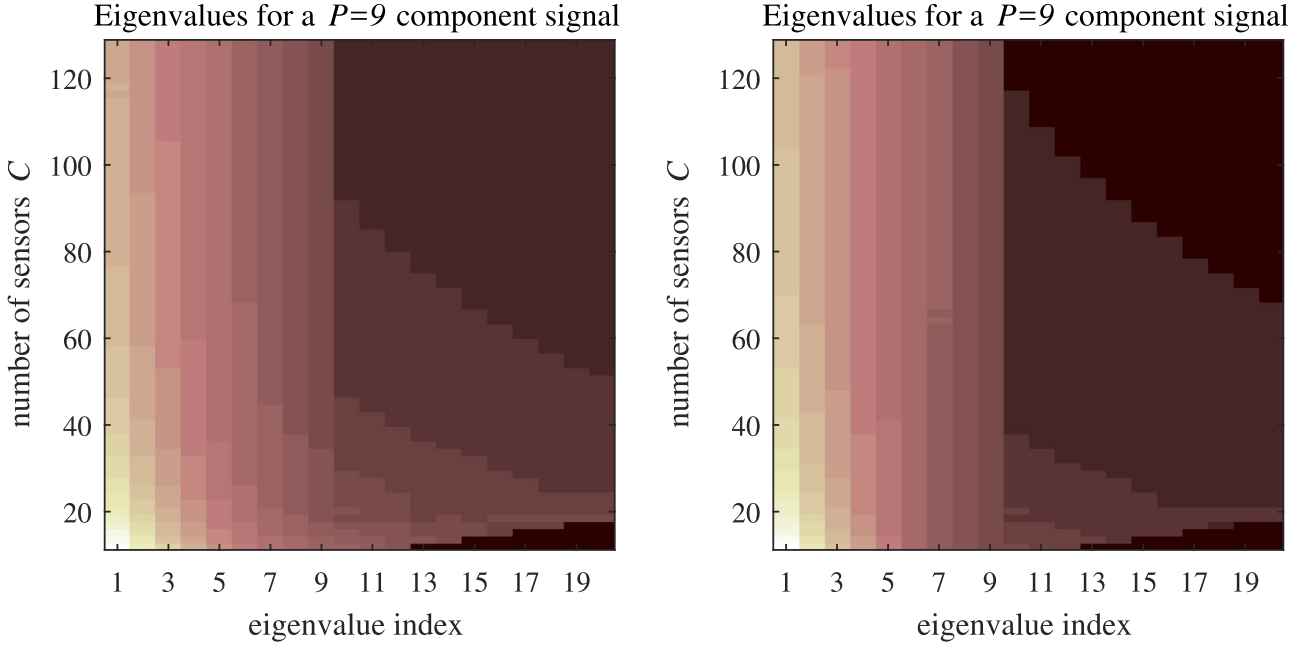


**Fig. 10.** Eigenvalues for a $P = 9$ component noisy signal averaged over 1000 random realizations, for two additive noise scenarios with $\sigma_\varepsilon^2 = 1$ (left) and $\sigma_\varepsilon^2 = 1/2$ (right). The indicator of a successful reconstruction is the gap between the eigenvalues for the eigenvectors at the eigenvalue index equal to $P = 9$ (representing the smallest energy of a combination of the signal components) and eigenvalue index equal to $P + 1 = 10$ (representing the strongest background noise component).

## 5. Conclusion

This work presents new contributions to the most challenging topic in multicomponent signal decomposition, that is, the case with components for which the supports are overlapped in the time-frequency plane. The decomposition concepts have been investigated starting directly from the signal autocorrelation matrix of the input, whose eigenvectors can be linearly combined to form individual signal components. The decomposition procedure based on the presented theory has been evaluated through several numerical examples, and has conclusively verified the presented theory and the decomposition efficacy. For rigor, the robustness of the procedure against the influence of an additive noise has been studied from the perspective of the degrees of freedom, that is, the number of sensors (channels) required to achieve a stable separation of signal components.

## Declaration of Competing Interest

The authors declare that they have no known competing financial interests or personal relationships that could have appeared to influence the work reported in this paper.

## Acknowledgment

The first author, Prof. Ljubiša Stanković, is thankful to Prof. Johann Böhme for continuous support over the years, during his stay at the Ruhr University in Bochum and subsequent joint research projects. Great-expert and friendly-warm support from Johann and Ulla Böhme had been of crucial importance to Stanković and his family during difficult period in former Yugoslavia.

## References

[1] L. Stanković, D. Mandic, M. Daković, M. Brajović, Time-frequency decomposition of multivariate multicomponent signals, Signal Process. 142 (January) (2018) 468–479, doi:10.1016/j.sigpro.2017.08.001.
[2] L. Stanković, M. Brajović, M. Daković, D. Mandic, Two-component bivariate signal decomposition based on time-frequency analysis, in: 22nd International Conference on Digital Signal Processing IEEE DSP 2017, pp. 23–25. August, London, United Kingdom.
[3] M. Brajović, L. Stanković, M. Daković, D. Mandic, Additive noise influence on the bivariate two-component signal decomposition, in: 7th Mediterranean Conference on Embedded Computing, MECO 2018, 2018. Budva, Montenegro, June.
[4] L. Stanković, T. Thayaparan, M. Daković, Signal decomposition by using the s-method with application to the analysis of HF radar signals in sea-clutter, IEEE Trans. Signal Process. 54 (Nov 11) (2006) 4332–4342.
[5] Y. Wei, S. Tan, Signal decomposition by the s-method with general window functions, Signal Process. 92 (January 1) (2012) 288–293.
[6] Y. Yang, X. Dong, Z. Peng, W. Zhang, G. Meng, Component extraction for non-stationary multi-component signal using parameterized de-chirping and band–pass filter, IEEE SP Lett. 22 (9) (2015) 1373–1377.
[7] Y. Wang, Y. Jiang, ISAR imaging of maneuvering target based on the l-class of fourth-order complex-lag PWVD, IEEE Trans. Geosci. Remote Sens. 48 (March 3) (2010) 1518–1527.
[8] I. Orović, S. Stanković, A. Draganić, Time-frequency analysis and singular value decomposition applied to the highly multicomponent musical signals, Acta Acustica United Acustica 100 (2014) 1.
[9] L. Stanković, M. Daković, T. Thayaparan, Time-Frequency Signal Analysis with Applications, Artech House, 2013. Mar.
[10] B. Boashash, Time-Frequency Signal Analysis and Processing – a Comprehensive Reference, Elsevier Science, Oxford, 2003.
[11] P. Flandrin, Time-Frequency/Time-Scale Analysis,, Academic press, 1998. Vol. 10.
[12] Z.M. Hussain, B. Boashash, Adaptive instantaneous frequency estimation of multicomponent FM signals using quadratic time-frequency distributions, IEEE Trans. Signal Process. 50 (Aug 8) (2002) 1866–1876.
[13] P.L. Shui, H.Y. Shang, Y.B. Zhao, Instantaneous frequency estimation based on directionally smoothed pseudo-Wigner-Ville distribution bank, IET Radar Sonar Navig. 1 (Aug 4) (2007) 317–325.
[14] B. Barkat, B. Boashash, Instantaneous frequency estimation of polynomial FM signals using the peak of the PWVD: statistical performance in the presence of additive gaussian noise, IEEE Trans. Signal Process. 47 (Sept 9) (1999) 2480–2490.
[15] S.C. Sekhar, T.V. Sreenivas, Auditory motivated level-crossing approach to instantaneous frequency estimation, IEEE Trans. Signal Process. 53 (April 4) (2005) 1450–1462.
[16] B. Boashash, Estimating and interpreting the instantaneous frequency of a signal. I. fundamentals, Proc. IEEE 80 (Apr 4) (1992) 520–538, doi:10.1109/5.135376.
[17] V. Katkovnik, L. Stanković, Instantaneous frequency estimation using the Wigner distribution with varying and data driven window length, IEEE Trans. Signal Process. 46 (Sep 9) (1998) 2315–2325.
[18] V.N. Ivanović, M. Daković, L. Stanković, Performance of quadratic time-frequency distributions as instantaneous frequency estimators, IEEE Trans. Signal Process. 51 (Jan 1) (2003) 77–89.
[19] A. Ahrabian, D. Looney, L. Stanković, D. Mandic, Synchrosqueezing-based time-frequency analysis of multivariate data, Signal Process. 106 (January) (2015) 331–341.
[20] G. Lopez-Risueno, J. Grajal, O. Yeste-Ojeda, Atomic decomposition-based radar complex signal interception, IEE Proc. - Radar Sonar Navig. 150 (Aug 4) (2003) 323–331. 1.
[21] J.C. Wood, D.T. Barry, Radon transformation of time-frequency distributions for analysis of multicomponent signals, IEEE Trans. Signal Process. 42 (Nov 11) (1994) 3166–3177.
[22] L. Stanković, M. Daković, T. Thayaparan, V. Popović-Bugarin, Inverse radon transform based micro-doppler analysis from a reduced set of observations, IEEE Trans. AES 51 (April 2) (2015) 1155–1169.
[23] M. Daković, L. Stanković, Estimation of sinusoidally modulated signal parameters based on the inverse radon transform, in: ISPA 2013, Trieste, Italy, 2013, pp. 302–307. 4-6 September.
[24] J.M. Lilly, S.C. Olhede, Analysis of modulated multivariate oscillations, IEEE Trans. Signal Process. 60 (Feb 2) (2012) 600–612.
[25] A. Omidvarnia, B. Boashash, G. Azemi, P. Colditz, S. Vanhatalo, Generalised phase synchrony within multivariate signals: an emerging concept in time-frequency analysis, in: IEEE International Conference on Acoustics, Speech and Signal Processing (ICASSP), 2012, pp. 3417–3420. Kyoto.
[26] J.M. Lilly, S.C. Olhede, Bivariate instantaneous frequency and bandwidth, IEEE Trans. Signal Process. 58 (Feb 2) (2010) 591–603.
[27] D.P. Mandic, N.u. Rehman, Z. Wu, N.E. Huang, Empirical mode decomposition-based time-frequency analysis of multivariate signals: the power of adaptive data analysis, IEEE Signal Process. Mag. 30 (Nov.) (2013) 74–86.
[28] S.M.U. Abdullah, N.u. Rehman, M.M. Khan, D.P. Mandic, A multivariate empirical mode decomposition based approach to pansharpening, IEEE Trans. Geosci. Remote Sens. 53 (July 7) (2015) 3974–3984.
[29] A. Hemakom, A. Ahrabian, D. Looney, N.u. Rehman, D.P. Mandic, Nonuniformly sampled trivariate empirical mode decomposition, in: IEEE International Conference on Acoustics, Speech and Signal Processing (ICASSP 2015), South Brisbane, QLD, 2015, pp. 3691–3695.
[30] G. Wang, C. Teng, K. Li, Z. Zhang, X. Yan, The removal of EOG artifacts from EEG signals using independent component analysis and multivariate empirical mode decomposition, IEEE J. Biomed. Health Inform. 20 (Sept 5) (2016) 1301–1308.
[31] S. Tavildar, A. Ashrafi, Application of multivariate empirical mode decomposition and canonical correlation analysis for EEG motion artifact removal, in: 2016 Conference on Advances in Signal Processing (CASP), Pune, 2016, pp. 150–154.
[32] Y. Zhang, M.G. Amin, B.A. Obeidat, Polarimetric array processing for nonstationary signals, in: S. Chandran (Ed.), Adaptive Antenna Arrays: Trends and Applications, Springer, 2004, pp. 205–218.
[33] M. Cobos, J.J. López, Stereo audio source separation based on timefrequency masking and multilevel thresholding, Digital Signal Process. 18 (6) (2008) 960–976.
[34] A. Omidvarnia, G. Azemi, P.B. Colditz, B. Boashash, A time-frequency based approach for generalized phase synchrony assessment in nonstationary multivariate signals, Digital Signal Process. 23 (3) (2013) 780–790.
[35] Z. Su, L. Ye, Processing of lamb wave signals, in Identification of Damage Using Lamb Waves. Lecture Notes in Applied and Computational Mechanics, vol 48, Springer, London, 2009.
[36] A. Belouchrani, K. Abed-Meraim, J.-F. Cardoso, E. Moulines, A blind source separation technique using second-order statistics, IEEE Trans. Signal Process. 45 (Feb 2) (1997) 434–444.
[37] A. Belouchrani, M.G. Amin, Blind source separation based on time-frequency signal representations, IEEE Trans. Signal Process. 46 (Nov 11) (1998) 2888–2897.
[38] A. Aissa-El-Bey, N. Linh-Trung, K. Abed-Meraim, A. Belouchrani, Y. Grenier, Underdetermined blind separation of nondisjoint sources in the time-frequency domain, IEEE Trans. Signal Process. 55 (March 3) (2007) 897–907.
[39] D. Gabor, Theory of communication. part 1: the analysis of information, J. Inst. Electr. Eng. - Part III 93 (26) (1946) 429–441.
[40] D. Wei, A.C. Bovik, On the instantaneous frequencies of multicomponent AM-FM signals, IEEE Signal Process. Lett. 5 (April 4) (1998) 84–86.
[41] J. Brown, Analytic signals and product theorems for hilbert transforms, IEEE Trans. Circuits Syst. 21 (November 6) (1974) 790–792.
[42] D. Vakman, L.A. VaÄshteÄ n, Amplitude, phase, frequencyfundamental concepts of oscillation theory, Sov. Phys. Uspekhi 20 (12) (1977) 1002–1016.
[43] A.H. Nuttall, E. Bedrosian, On the quadrature approximation to the hilbert transform of modulated signals, Proc. IEEE 54 (Oct 10) (1966) 1458–1459.
[44] A.W. Rihaczek, E. Bedrosian, Hilbert transforms and the complex representation of real signals, Proc. IEEE 54 (March 3) (1966) 434–435.

[45] B. Picinbono, On instantaneous amplitude and phase of signals, IEEE Trans. Signal Process. 45 (March 3) (1997) 552–560.
[46] L. Stanković, A measure of some time–frequency distributions concentration, Signal Process. 81 (2001) 621–631.
[47] W. Hu, K. Wu, P.P. Shum, N.I. Zheludev, C. Soci, All-optical implementation of the ant colony optimization algorithm, Sci. Rep, 6 (2016), doi:10.1038/srep26283.
[48] R. Chelouaha, P. Siarry, Genetic and neldermead algorithms hybridized for a more accurate global optimization of continuous multiminima functions, Eur. J. Oper. Res. 148 (July 2) (2003) 335–348. 16.
[49] S. Kirkpatrick, C.D. Gelatt, M.P. Vecchi, Optimization by simulated annealing, Science 220 (4598) (1983) 671–680, doi:10.1126/science.220.4598.671. 13 May.
[50] A. Neumaier, Complete search in continuous global optimization and constraint satisfaction, Acta Numerica 13 (1) (2004).
[51] J.C. Spall, Introduction to Stochastic Search and Optimization, Wiley, ISBN 0-471-33052-3.
[52] J. Larson, S.M. Wild, A batch, derivative-free algorithm for finding multiple local minima, Optim. Eng. 17 (March 1) (2016) 205–228, doi:10.1007/s11081-015-9289-7.
[53] A. Cichocki, S. Amari, Adaptive Blind Signal and Image Processing: Learning Algorithms and Applications, John Wiley and Sons, 2002. Vol. 1 pp. 191–193.